Resonant interband tunnel diodes with AlGaSb barriers

R. Magno,[a] A. S. Bracker, and B. R. Bennett

Naval Research Laboratory, Washington, DC 20375-5347

The peak current density of InAs/AlSb/GaSb/AlSb/InAs resonant interband tunneling diodes has been enhanced by replacing the AlSb barriers with $Al_{1-x}Ga_xSb$ that has a narrower band gap. The devices were grown by molecular beam epitaxy and tested at room temperature. Diodes with nominally identical 7-ML-thick ternary alloy barriers with $x=0.35$ are found to have peak current densities three times larger than those with AlSb barriers. The peak-to-valley current ratio decreases by only one third from 18 for the AlSb diodes to 12 for diodes with the ternary alloy barriers. [DOI: 10.1063/1.1365940]

Resonant interband tunneling diodes (RITDs) in the InAs/AlSb/GaSb materials system[1] are of interest for applications in highly functional, low power logic circuits capable of operating at frequencies approaching 100 GHz.[2–4] Because the negative resistance peak occurs near 100 meV in this material system, it may be possible to produce logic circuits with lower power consumption than those made with other material systems.[2] High speed applications require diodes with a peak current density, I_p, in the range of 10^5 A/cm^2 and a large peak-to-valley current ratio (P/V) to minimize power dissipation. This communication reports on an experimental test of the use of $Al_{1-x}Ga_xSb$ alloy barriers, which enhance the peak current densities of RITDs. The associated changes in the valley current are also discussed, as a large increase in the peak current is of little use if it is accompanied by a large increase in the valley current.

The inset in Fig. 1(a) illustrates the material and band structure of a RITD. Starting at the right and left sides of the diagram are the narrow band gap InAs electrodes. Inside these layers are wide band gap AlSb tunnel barriers, and finally inside the barriers is a GaSb well. An electron in the conduction band (CB) of an InAs electrode tunnels through the band gap of an AlSb barrier into the valence band (VB) of the GaSb well, through the second AlSb barrier into the CB of the other InAs electrode. This band structure results in high peak current densities, and large peak-to-valley current ratios at biases near 100 meV at room temperature.

The tunneling barrier thickness and barrier height are key parameters in determining I_p in tunnel diodes, and for RITDs with 3 ML AlSb barriers I_p is near 4×10^4 A/cm^2. The factors determining the P/V ratio are not as well understood, but P/V ≈ 8 is typical for RITDs with 3 ML AlSb barriers.[5–10] Higher current densities are expected with thinner barriers as I_p increases exponentially with decreasing barrier thickness. Simply decreasing the barrier thickness becomes problematic in terms of reproducibility from growth to growth and across a wafer in one growth as the barrier thickness approaches 3 ML or less. An alternate and as yet not experimentally explored approach to increasing I_p is to reduce the barrier height by using $Al_{1-x}Ga_xSb$ alloy barriers

that have a narrower band gap than AlSb. This approach offers the possibility of obtaining high current densities with thicker barriers that are easier to grow with a high degree of reproducibility.

Lapushkin, Zakharova, and Gergel, in a theoretical article on interband tunneling, predicted that improvements in I_p could be obtained by using $Al_{1-x}Ga_xSb$ alloys rather than AlSb for the barriers.[11] The theory predicts that a diode with 25-Å-thick alloy barriers with $x=0.4$ and a 65 Å well will have $I_p=2 \times 10^4$ A/cm^2 and P/V$=20$ at room temperature. The theory also predicts $I_p=2 \times 10^3$ A/cm^2 and P/V$=9$ for the same geometry with AlSb barriers. These numbers suggest that a factor of 20 increase in I_p and a doubling of the P/V ratio may be obtained by using alloy barriers. The predictions listed above for a diode with AlSb barriers compare well with values of $I_p=1.3 \times 10^3$ A/cm^2 and P/V$=18$ measured by us for a device with 8 ML (24 Å) AlSb barriers, and a 27 ML (81 Å) GaSb well. Alloy barriers also offer a tool for checking the validity of this and other tunneling models.[11–16] By varying the Ga content in the barrier it is possible to move both the conduction and valence band edges in the barrier relative to the band edges of the InAs electrodes and GaSb well.

The use of $Al_{1-x}Ga_xSb$ has an additional advantage over AlSb, as it is more closely lattice matched to the GaSb and InAs used in the diodes. This could have a positive effect on the P/V ratio by reducing the number of strain-induced defects that are likely to increase the valley current.[8,10]

Some preliminary work exploring the use of $Al_{1-x}In_xSb$ barriers is also presented. $Al_{1-x}In_xSb$ alloy barriers also have a narrower band gap than AlSb, and their use is expected to increase I_p, but the experiments need to be done to determine the amount of improvement. $Al_{1-x}In_xSb$ barriers will have a larger lattice mismatch than AlSb barriers with the other components of the diodes, and the additional strain is expected to make it more difficult to grow barriers free of defects that add to the valley current.

The diodes examined here were grown by molecular beam epitaxy on InAs substrates. A buffer layer consisting of 1 μm of n^+ InAs (3×10^{18} Si cm^{-3}) was grown first. The RITD structure, as illustrated by the inset in Fig. 1(a), consists of a pair of nominally identical $Al_{1-x}Ga_xSb$ barriers

---

[a] Electronic mail: Magno@bloch.nrl.navy.mil
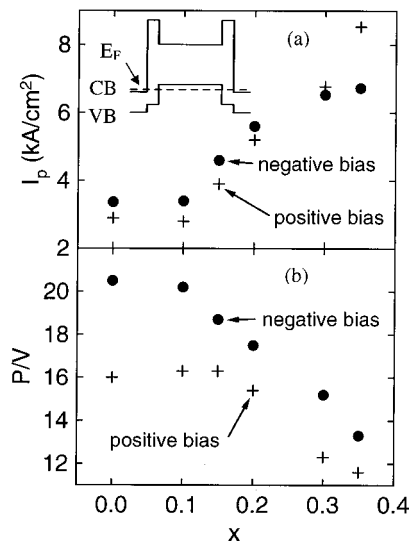
FIG. 1. (a) Dependence of the peak current density on the Ga fraction for samples with nominally identical 7-ML-thick $Al_{1-x}Ga_xSb$ barriers, (b) P/V ratio for the samples. The inset in (a) indicates the conduction band, CB, valence band, VB, and Fermi energy, E_F, of an interband tunnel diode.

FIG. 2. (a) Dependence of the peak current density on the Ga fraction for samples with nominally identical 10-ML-thick $Al_{1-x}Ga_xSb$ barriers, (b) P/V ratio for the samples. The lines are guides to the eye.

sandwiching a 27 ML GaSb well. The InAs 40 ML (12 nm) layers adjacent to both AlSb barriers were undoped, and the next 30 nm InAs layers away from the barriers were doped with 1×10^{17} Si cm^{-3}. Finally, a 200 nm layer of 3×10^{18} Si cm^{-3} InAs was grown on top of the RITD. Growth procedures were used to form InSb interface bonds at the InAs/AlSb interfaces. Reflection high-energy electron diffraction (RHEED) measurements were used to calibrate growth rates in order to determine the thicknesses of the RITD layers. Sample temperatures during growth were 400 °C. The temperature was monitored by a thermocouple, calibrated by observing the InAs $(2\times4)\rightarrow(4\times2)$ transition in RHEED. The temperature of the Ga and Al sources were set to have a barrier growth rate of 0.5 ML/s. As only one Ga source was used, this set the growth rate for the GaSb well, but this is not expected to have a significant impact. Standard photolithography techniques were used to pattern Ti/Pt/Au ohmic contacts with diameters ranging from 2 to 50 μm. Mesas were formed by using the ohmic contacts as the etch stop in a wet etching process. Current–voltage ($I–V$) measurements were made at room temperature by tensioning a fine gold wire point contact against the ohmic contact. In the data plots, ''positive bias'' means the top of the mesa is biased positively with respect to the substrate. The data represent average values for several mesas measured on a chip.

The current densities and P/V ratios for a series of samples with nominally identical top and bottom barriers either 7 or 10 ML thick are shown in Figs. 1 and 2, respectively. Data for both bias polarities are presented, as the differences are useful in evaluating the growth procedures that may result in barrier roughness[17] and Ga segregation[17] phenomena. In both figures the peak current density increases by almost a factor of 3 with increasing x, although the threefold increase occurs at a smaller Ga concentration for the 10 ML sample compared to the 7 ML one. The current has a threshold near $x \approx 0.1$ where it begins to increase for the 7 ML
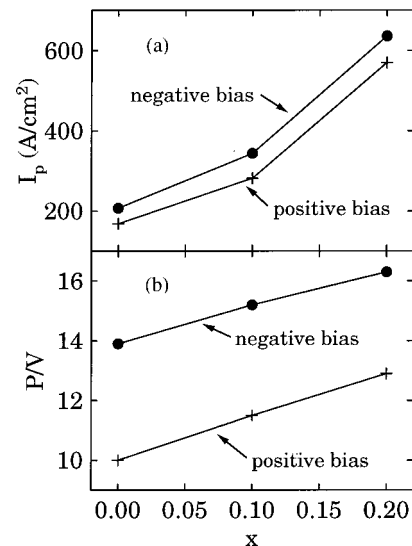
data, while no threshold is found for the 10 ML data. The peak currents are slightly asymmetric with the negative bias peak currents being larger than the positive bias except for the 7 ML data at $x = 0.35$ where the asymmetry in the peak currents changes with the positive bias current becoming larger than the negative bias current. These asymmetries indicate a higher tunneling probability for one barrier compared to the other due to differences in the growth even though an effort was made to make them identical.

The peak-to-valley current ratios for the 7 and 10 ML samples exhibit different behavior as the Ga fraction in the barrier increases. P/V increases with increasing x for the 10 ML samples, while it is constant for the 7 ML samples for $x \leqslant 0.1$ and decreases for larger values of x. The most significant difference occurs in the 7 ML P/V data for $x \leqslant 0.1$ where P/V ≈ 20 for negative bias and 16 for positive. Near $x \approx 0.1$ the P/V ratio converges and decreases linearly reaching about 12 at $x = 0.35$ with the negative bias ratio being the larger one. It is important to note that while the peak current density increases by almost a factor of 3, the P/V ratio only decreases by about one third to 12 for the 7 ML samples. This is still a reasonably large value. It is not understood why P/V increased for the 10 ML data but decreased for the 7 ML data. As noted above, for a diode similar to the 7 ML one reported here, the model by Lapushkin and co-workers predicts twofold improvement in P/V on going from $x = 0$ to $x = 0.4$.[11] The thickness dependence of the P/V ratio for diodes with AlSb barriers has a maximum near 7 ML suggesting that the mechanism that dominates the valley current for thick barriers is different from the one that dominates for thin barriers.[8]

Some results for $Al_{1-x}In_xSb$ barrier devices are shown in Fig. 3. The asymmetry in the $I–V$ reflects the fact that the bottom barrier in this device is 7 ML of AlSb and the top one is 7 ML of $Al_{0.8}In_{0.2}Sb$. The In alloy was only used for the top barrier as the InSb lattice constant is larger than the InAs

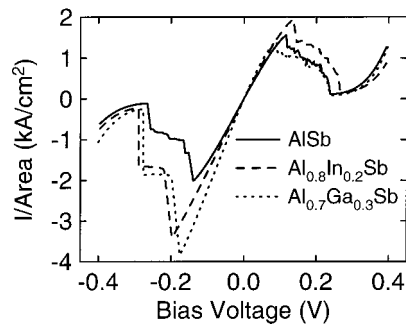J. Appl. Phys., Vol. 89, No. 10, 15 May 2001

Magno, Bracker, and Bennett   5793

FIG. 3. Comparison of the $I-V$ for three samples with similar 7 ML AlSb bottom barriers, and with top barriers of either AlSb (solid line) or $Al_{0.8}In_{0.2}Sb$ (long dashed line) or $Al_{0.7}Ga_{0.3}Sb$ (short dashed line).

lattice constant and using the alloy in the lower barrier may have introduced undesirable strain effects resulting in defects in the RITD layers. To judge the effect of the $Al_{0.8}In_{0.2}Sb$, a sample with nominally identical 7 ML AlSb barriers and one with a 7 ML AlSb bottom barrier and a 7 ML $Al_{0.7}Ga_{0.3}Sb$ top barrier are also shown in Fig. 3. Table I contains a comparison of the peak current densities and P/V ratios for the three samples. The most significant increase in current for both alloy barriers is found for negative bias with I_p for the $Al_{0.8}In_{0.2}Sb$ diode almost as large as that found for the 30% Ga one. The positive bias peak current for the In alloy barrier is somewhat larger than the current for the AlSb control sample. This is different from behavior found for the Ga alloy barrier, which has nearly the same peak current as the AlSb barrier device. The negative bias P/V ratio for the In alloy barrier is comparable to that for the Ga alloy barrier but somewhat lower than that for the AlSb diode. These results suggest that $Al_{1-x}In_xSb$ barriers may also offer a means of

achieving higher peak current densities with acceptable valley currents.

In summary, $Al_{1-x}Ga_xSb$ has been used to replace wider band gap AlSb barriers in InAs/GaSb/AlSb interband tunneling diodes. The use of these narrow band gap alloys has resulted in a threefold increase in the peak current density compared to diodes with AlSb barriers. The threefold current improvement is obtained at $x=0.35$ for diodes with 7 ML alloy barriers and at the smaller value of $x=0.2$ for diodes with 10 ML barriers. The P/V ratio for the 7 ML alloy devices decreased to 12, which is still a reasonable value for possible applications. Interestingly, the P/V increased with increasing Ga concentration in the 10 ML diodes. Preliminary results have demonstrated the possibility of using $Al_{1-x}In_xSb$ barriers.

TABLE I. Peak current densities, I_p, and P/V ratios for negative, $-$, and positive, $+$, bias for samples shown in Fig. 3.

Top barrier	P/V$_-$	I_{p^-} (kA/cm^2)	P/V$_+$	I_{p^+} (kA/cm^2)
AlSb	17.9	2	13.5	1.5
$Al_{0.8}In_{0.2}Sb$	15.6	3.4	12.7	1.9
$Al_{0.7}Ga_{0.3}Sb$	15.6	3.9	15	1.4

[1] J. R. Söderström, D. H. Chow, and T. C. McGill, Appl. Phys. Lett. **55**, 1094 (1989).
[2] K. J. Chen, K. Maezawa, and M. Yamamoto, IEEE Electron Device Lett. **17**, 127 (1996).
[3] P. Mazumder, S. Kulkarni, M. Bhattacharya, J. Ping Sun, and G. I. Haddad, Proc. IEEE **86**, 664 (1998).
[4] B. R. Bennett, A. S. Bracker, R. Magno, J. B. Boos, R. Bass, and D. Park, J. Vac. Sci. Technol. B **18**, 1650 (2000).
[5] J. Shen, J. Appl. Phys. **78**, 6220 (1995).
[6] K. Shiralagi, J. Shen, and R. Tsui, J. Electron. Mater. **26**, 1417 (1997).
[7] H. Kitabayashi, T. Waho, and M. Yamamoto, J. Appl. Phys. **84**, 1460 (1998).
[8] R. Magno, A. S. Bracker, B. R. Bennett, M. E. Twigg, and B. D. Weaver, Proceedings of the 2000 International Conference on Indium Phosphide and Related Materials, 2000, p. 122.
[9] B. Z. Nosho, W. H. Weinberg, W. Barvosa-Carter, A. S. Bracker, R. Magno, B. R. Bennett, J. C. Culbertson, B. V. Shanabrook, and L. J. Whitman, J. Vac. Sci. Technol. B **17**, 1786 (1999).
[10] R. Magno, B. D. Weaver, A. S. Bracker, and B. R. Bennett, Appl. Phys. Lett. (to be published).
[11] I. Lapushkin, A. Zakharova, and V. Gergel, Semicond. Sci. Technol. **14**, 731 (1999).
[12] D. Z.-Y. Ting, E. T. Yu, and T. C. McGill, Phys. Rev. B **45**, 3583 (1992).
[13] M. S. Kiledjian, J. N. Schulman, K. L. Wang, and K. V. Rousseau, Phys. Rev. B **46**, 16012 (1992).
[14] J. Genoe, K. Fobelets, C. Van Hoof, and G. Borghs, Phys. Rev. B **52**, 14025 (1995).
[15] I. Lapushkin, A. Zakharova, V. Gergel, H. Goronkin, and S. Tehrani, J. Appl. Phys. **82**, 2421 (1997).
[16] J. N. Schulman, Solid-State Electron. **43**, 1367 (1999).
[17] R. Magno, A. S. Bracker, B. R. Bennett, B. Z. Nosho, M. E. Twigg, and L. J. Whitman (unpublished).